Enhanced Nickel-Seeded Synthesis of Germanium Nanowires

ARTICLE *in* CHEMISTRY OF MATERIALS · MAY 2013

Impact Factor: 8.35 · DOI: 10.1021/cm401047w

5 AUTHORS, INCLUDING:

Xiaotang Lu
University of Texas at Austin
15 PUBLICATIONS **392** CITATIONS
SEE PROFILE

Aaron Chockla
University of Texas at Austin
17 PUBLICATIONS **611** CITATIONS
SEE PROFILE

CHEMISTRY OF MATERIALS

Article

pubs.acs.org/cm

Enhanced Nickel-Seeded Synthesis of Germanium Nanowires

Xiaotang Lu, Justin T. Harris, Julián E. Villarreal, Aaron M. Chockla, and Brian A. Korgel*

Department of Chemical Engineering, Texas Materials Institute, Center for Nano- and Molecular Science and Technology, The University of Texas at Austin, Austin, Texas 78712, United States

Supporting Information

ABSTRACT: Germanium (Ge) nanowires can be grown using either gold (Au) or nickel (Ni) seeds in a supercritical solvent; however, the quality and yield of the nanowires is much higher using Au seeds and diphenyl germane (DPG) as a reactant under typical reaction conditions. We find that the addition of monophenylsilane (MPS) dramatically improves the yield and quality of Ni-seeded Ge nanowires, producing straight nanowires with relatively uniform diameter and nearly 100% conversion of DPG to Ge. MPS participates in the phenyl redistribution reaction of DPG and serves as a phenyl sink that speeds DPG decomposition and increases the conversion to Ge to nearly 100%. MPS addition to Au-seeded nanowire reactions also increases the DPG conversion to Ge to nearly 100% and improves the nanowire quality at higher growth temperature.

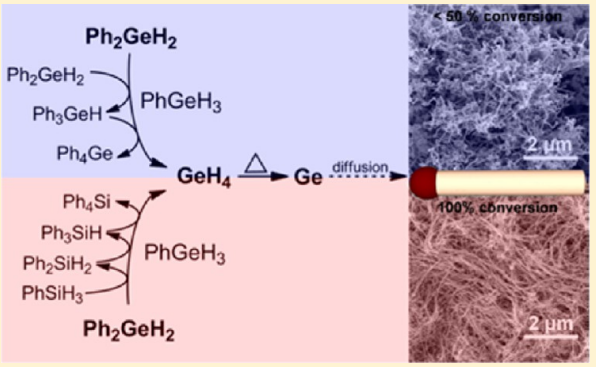

KEYWORDS: *germanium, nanowires, germanes, silanes, SFLS, SFSS, colloid chemistry*

INTRODUCTION

Semiconductor nanowires have been proposed for many uses, including thermoelectrics, thin film transistors, chemical sensors, photovoltaics, as semiconducting fabric, membranes, and lithium ion battery electrodes, which often require large quantities of nanowires at reasonable cost.[1] Solution-based approaches of solution−liquid−solid (SLS)[2−4] and supercritical fluid−liquid−solid (SFLS)[5,6] growth provide versatile synthetic routes to semiconductor nanowires with tunable size and a wide range of compositions, including Si,[7,8] Ge,[9,10] III−V,[11−14] IV−VI,[15] and II−VI[16−22] compounds, and even ternary $CuInSe_2$.[23,24] These methods rely on the use of metal particles to seed nanowire growth, usually at reaction temperatures exceeding a metal-semiconductor eutectic similar to vapor−liquid−solid (VLS)[25,26] growth in the gas phase. For Ge nanowires, Au has been the most widely used seed metal for VLS and SFLS growth.[9,27−40] It forms a relatively low temperature eutectic with Ge (361 °C),[41] induces the growth of high quality nanowires, and is chemically inert. Au, however, is a relatively expensive metal and creates electronic traps in Ge.[42] Therefore, a variety of other seed metals have been explored to grow Ge nanowires, including Ni,[43−47] Co,[44] Cu,[44,48−50] Mn,[44] Fe,[44] Bi,[10] Ag,[51] and stainless steel.[52] However, there have been few direct comparisons of how these different seed metals influence nanowire growth.

In our own search for a good alternative seed metal for Ge nanowires, we have observed significant differences between Au and Ni seeding of Ge nanowire growth in supercritical fluids. Au appears to *catalyze* the decomposition of the reactant diphenylgermane (DPG),[53] whereas Ni does not. The supercritical reaction temperatures (<625 °C) are well below the Ni/Ge eutectic temperature of 762 °C, and nanowire growth occurs through a *solid* phase seed, which can significantly influence the quality of the nanowires.[43,46] Comparatively, Ni is a relatively poor seed metal compared to Au under typical growth conditions. However, we discovered that greatly enhanced DPG decomposition by addition of monophenylsilane (MPS) to the reaction can lead to extremely high quality Ge nanowires from Ni seeds with very high product yields, approaching 100% conversion of DPG to Ge. MPS is a typical reactant for solution-based growth of Si nanowires[5,8,54−59] but is employed here only as a phenyl group scavenger that does not participate in the growth reaction. Here, we report these findings.

EXPERIMENTAL SECTION

Materials. Anhydrous toluene (99.8%) was purchased from Sigma-Aldrich, diphenylgermane (DPG) and phenylsilane (MPS) were purchased from Gelest. Hydrogen tetrachloroaurate(III) trihydrate (≥99.9%), tetraoctylammonium bromide (98%), and sodium borohydride (≥98.0%) were purchased from Aldrich. Nickel(acetylacetonate)$_2$ (95%), trioctylphosphine (90%), and oleylamine (70%) were purchased from Aldrich. All chemicals were used as received.

Gold (Au) nanocrystals averaging 2 nm in diameter were prepared by Brust's method.[60] (See the Supporting Information for experimental details and transmission electron microscopy (TEM) characterization, Figure S1a). Nickel (Ni) nanocrystals averaging 4 nm in diameter were prepared by Hyeon's method.[61] (See the Supporting

Received: April 1, 2013
Revised: April 27, 2013
Published: May 2, 2013

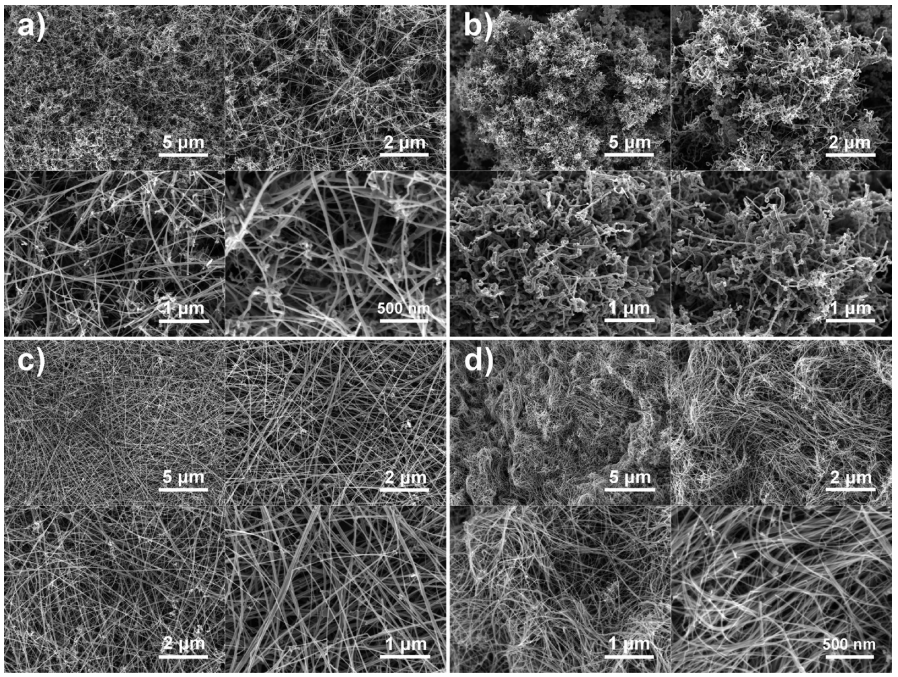

Figure 1. SEM images of Ge nanowires formed at 500 °C with (a) Au nanocrystal seeds; (b) Ni nanocrystal seeds; (c) Au nanocrystal seeds with addition of MPS; and (d) Ni nanocrystal seeds with addition of MPS.

Information for experimental details and TEM characterization, Figure S1b).

Germanium Nanowire Synthesis. Ge nanowires were synthesized in a 10 mL titanium tubular reactor connected to a high pressure liquid chromatography (HPLC) pump, as previously described.[62] Au-seeded Ge nanowires were synthesized with a 28 mL reactant solution of 3.6 mg/L Au nanocrystals and 7.3 mM DPG in anhydrous toluene prepared in a nitrogen-filled glovebox. Ni-seeded Ge nanowires were made using a 28 mL reactant solution of 5 mg/L Ni nanocrystals and 7.3 mM DPG in anhydrous toluene prepared in the glovebox. Nanowires were also made by adding 7.3 mM MPS to the reactant solutions. Prior to precursor injection, the 10 mL titanium tubular reactor was filled with N_2 in the glovebox and then connected to the six-way valve and the back-pressure regulator at two ends. After the reactor was preheated to 500 °C and pressurized to 10.3 MPa with anhydrous toluene, nanowire growth was carried out with the reactant solution fed into the reactor at a rate of 0.5 mL/min for 40 min. The outlet pressure was maintained at 10.3 MPa. After completing the injection of the reactants, the reactor was sealed and removed from the heating block. The effluent was also collected during each reaction. After the reactor cools to room temperature, the nanowire product was collected and washed with a mixture of 4 mL of chloroform, 2 mL of toluene, and 2 mL of ethanol, followed by centrifugation at 8000 rpm for 5 min. The purification procedure was repeated three times to remove unreacted reagent and molecular byproducts.

Materials Characterization. Scanning electron microscopy (SEM) images were acquired on a Zeiss Model SUPRA 40 VP SEM with an in-lens arrangement, a working voltage of 5.0 kV and a working distance of 5 mm. The SEM samples were prepared by drop-casting Ge nanowires onto silicon wafers and drying.

Low-resolution transmission electron microscopy (TEM) images were acquired on a FEI Tecnai Spirit Bio Twin operated at 80 kV. High-resolution transmission microscopy (HRTEM) images were acquired on a field emission JEOL 2010F TEM operated at 200 kV. TEM samples were prepared by drop-casting 5 μL of dilute Ge nanowire dispersion in chloroform onto a 200 mesh copper lacey carbon TEM grid (Electron Microscopy Science).

X-ray diffraction (XRD) was performed on a Rigaku R-Axis Spider diffractometer with an image plate detector using Cu Kα radiation (λ = 1.54 Å) and a graphite monochromator. XRD samples were prepared by mixing a small amount of dried Ge nanowires with a droplet of mineral oil and mounting the mixture on a nylon loop.

Gas chromatography–mass spectrometry (GC-MS) data were obtained using a Thermo TraceGC interfaced to a Thermo TSQ triple quadrupole mass spectrometer operating in positive CI mode, with methane as the reagent gas. Samples were injected in splitless mode onto a Restek Rxi-5Sil MS column (30 m, 0.25 mm ID, 0.25 μm) with an injector temperature of 280 °C and separated at a constant flow of helium (1.2 mL/min) by ramping temperature from 40 to 320 °C at 30 °C/min.

RESULTS

Ge Nanowires Grown with Au vs Ni Seeds. We directly compared Ge nanowire growth in supercritical toluene using DPG as a reactant using Au and Ni nanocrystals as seeds. The optimum reaction temperature for SFLS growth of Ge nanowires from DPG using Au seeds is 380 °C.[33,62,63] Reactions at 380 °C using Ni seeds did not yield any nanowires and produced only microspheres and rods (see the Supporting Information, Figure S2). It was necessary to raise the reaction temperature to 500 °C to produce any Ge nanowires with Ni seeds. However, even at the relatively high temperature of 500 °C, the yield and quality of Ge nanowires were poor. Figures 1a and 1b show SEM images of typical Ge nanowire product grown with Au and Ni seeds in supercritical toluene with DPG at 500 °C. Although Ge nanowires grown with Au seeds at 500 °C are not as pristine as those grown at 380 °C due to more severe agglomeration of Au seeds and secondary growth of Ge on the existing Ge nanowires, the nanowires are still mostly straight and long with high aspect ratio and diameters ranging between 10 and 40 nm. In contrast, the Ni-seeded Ge nanowires are highly kinked and relatively short with low reaction product yield (20% conversion of DPG to Ge).

MPS Addition. The addition of monophenylsilane (MPS) to the DPG reaction with Ni nanocrystals greatly increases the quality of Ge nanowires. See, for example, the SEM images in

dx.doi.org/10.1021/cm401047w | Chem. Mater. 2013, 25, 2172–2177

Figure 1d of the Ni-seeded Ge nanowires grown with addition of MPS. The nanowires are long and straight with average diameter of 14 nm and a relatively narrow diameter distribution. The reaction yield of the Ni-seeded nanowires is also very high with a conversion of DPG to Ge of 92%. The improvement in quality and yield of product is dramatic.

MPS also improves the yield and quality of the Au-seeded reactions carried out at high temperature, as shown in the SEM images in Figure 1a and c. The Au-seeded nanowires grown with MPS are noticeably straighter than those made without MPS, and the reaction yields are significantly higher. The Au-seeded Ge nanowires made at the higher temperature of 500 °C have similar quality as those made without MPS under optimized conditions at 380 °C. The yield of the reaction with MPS at 500 °C increases to nearly 100% from 30%, which represents a significant advance in this synthetic approach. Table 1 summarizes the yield of the various Ge nanowire growth reactions.

Table 1. Molar Conversion of DPG to Ge Nanowire Product for Reactions in Supercritical Toluene at 500 °C Involving Au and Ni Seeds with and without Added MPS[a]

reaction	DPG conversion (%)
Au seeds, no MPS	30.1
Ni seeds, no MPS	20.4
Au seeds, with MPS	93.5
Ni seeds, with MPS	92.2

[a]The theoretical yield in the absence of MPS is 50%.[53]

Role of MPS. Figure 2 shows XRD data from Ge nanowires grown with Au and Ni seeds with and without MPS added. All

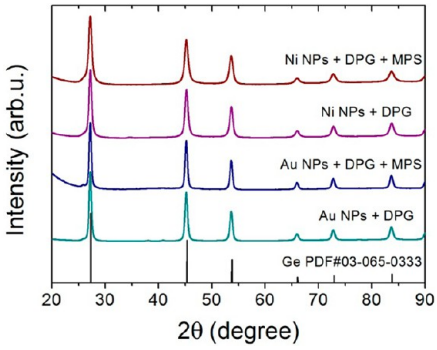

Figure 2. XRD of Ge nanowires made by decomposing DPG in supercritical toluene at 500 °C with either Au or Ni seeds with or without MPS added to the reaction. The seed particle and reactants are indicated beside each diffraction pattern. A reference pattern for diamond cubic Ge is provided (PDF No.: 03-065-0333).

of the XRD patterns indexed to diamond cubic Ge, indicating that MPS addition does not lead to significant Si incorporation into the nanowires; however, trace Si incorporation cannot be ruled out (see Figure S3 in the Supporting Information for EDS measurements and associated discussion). High resolution TEM determinations of the nanowire crystal structure and interplanar spacing are also consistent with diamond cubic Ge. Figure 3 shows examples of TEM images of Ge nanowires grown with Ni seeds and added MPS. Ni germanide alloy is found at the tips of the nanowires, similar to other Ni-seeded

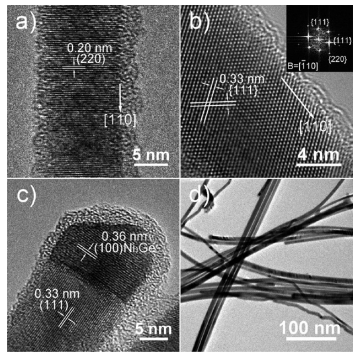

Figure 3. TEM images of Ge nanowires synthesized with Ni seeds and added MPS. (a) The core of a Ge nanowire with (220) fringes perpendicular to the [110] growth direction, (b) Ge nanowire showing crossed {111} fringes at 35° to the [110] growth direction. The inset shows the corresponding FFT pattern indexed to diamond cubic Ge, (c) Ge nanowires with Ni_3Ge at its tip. The *d*-spacing of 0.36 nm in the tip corresponds to the (100) planes of cubic Ni_3Ge. (PDF No.: 65-0142).

Ge nanowire growth studies.[43−47] The [110] growth direction is similar to other SFLS-grown Ge nanowires.[6,43,46,64]

There is no significant Si incorporation into the nanowires (i.e., Si−Ge alloying), and no separate Si diffraction peaks are detected either. This results implies that MPS is a spectator to nanowire growth, while significantly enhancing DPG decomposition kinetics. DPG decomposition proceeds by phenyl redistribution into germane and higher order phenylgermanes, triphenyl germane (TPG), and tetraphenyl germane (QPG).[53,65] The theoretical yield of Ge nanowires from DPG is only 50% because the TPG and QPG byproducts do not decompose,[64] explaining the low nanowire yields in Table 1 using DPG (without added MPS). Also, without MPS, the Au-seeded reactions have noticeably higher conversions of DPG to Ge nanowires than the Ni-seeded reactions. This is consistent with previous studies showing that Au has a catalytic effect on DPG decomposition.[53] Ni apparently does not play the same role.

When MPS was added, the Ge yield from DPG increases to more than 90%—both with Au and Ni seeds—which is well above the theoretical yield. At 500 °C, MPS also undergoes phenyl redistribution and decomposes typically to silane and tetraphenyl silane (QPS).[8,54] In the presence of DPG, it appears that phenylsilane becomes a phenyl sink, withdrawing phenyl groups from DPG to form higher order phenylsilanes while pushing the distribution of DPG decomposition products toward Ge. This reaction pathway is consistent with stronger Si−C bonding compared to Ge−C.[66]

Confirmation of Phenyl Redistribution Between DPG and MPS. The phenyl redistribution pathway between DPG and MPS was confirmed by GC-MS analyses of reactor effluent. Figure 4 shows the GC-MS data obtained from Au and Ni seeded reactions with and without MPS. Without MPS added to the reaction, unreacted DPG is detected, along with significant TPG. QPG is not detected because it is insoluble and accumulates in the reactor. More DPG was observed in the effluent from the Ni seeded reactions than the Au seeded reactions, consistent with the lower product yield in those reactions.

From reactions with MPS added, the predominant byproduct observed by GC-MS was TPS and very little TPG. Some unreacted DPG was still observed in the reactions with Ni

dx.doi.org/10.1021/cm401047w | Chem. Mater. 2013, 25, 2172−2177

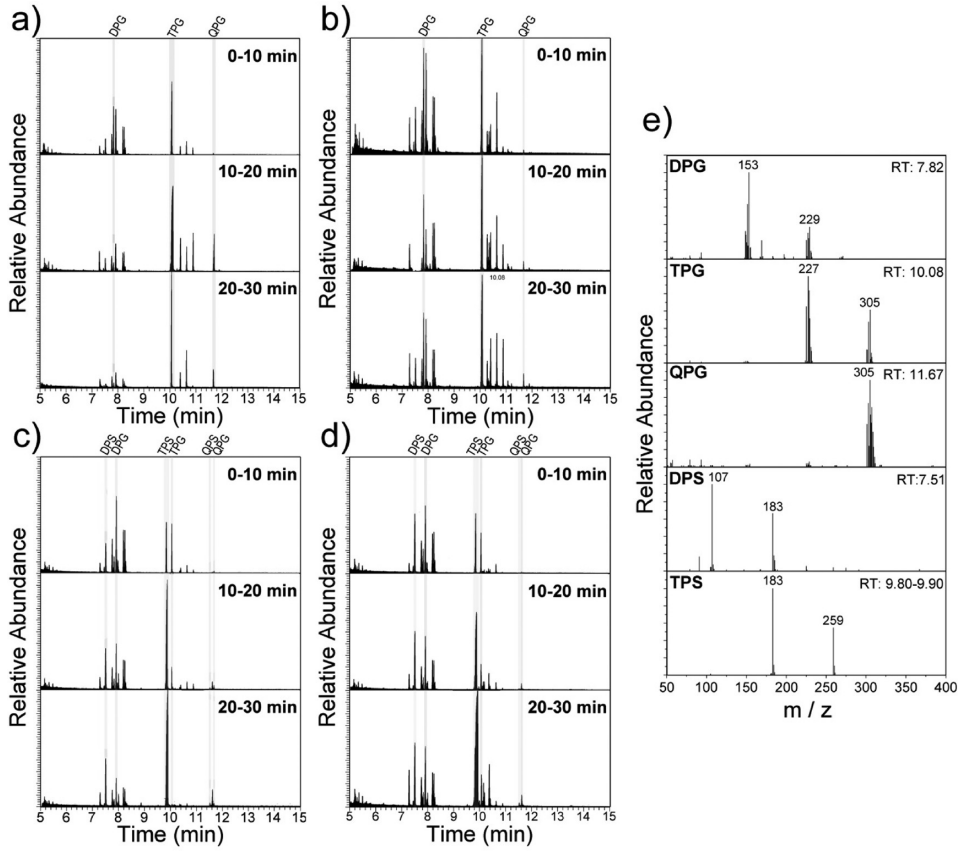

Figure 4. Gas chromatography spectra of effluents collected at different times during the Ge nanowire growth reactions using (a) Au (no MPS), (b) Ni (no MPS), (c) Au with MPS, (d) Ni with MPS. Peak heights have been normalized to the highest peak in each column. (e) Mass spectra of major byproducts in the reaction.[67]

seeds, consistent with the slightly lower yields using Ni than Au. These data confirm that MPS enhances DPG conversion to Ge by withdrawing phenyl groups, as illustrated in Figure 5a. With the addition of MPS, the theoretical yield becomes 100% as long as sufficient MPS is present (i.e., at least a 2:3 ratio of MPS to DPG).

DISCUSSION

Ni vs Au Seeding of Ge Nanowires. Ge nanowire growth is substantially different when seeded with Au than with Ni. One obvious difference between the two metals is their significantly different Au/Ge and Ni/Ge eutectic temperatures (Figure 5). Au-seeded growth occurs above the Au/Ge eutectic and Ge nanowires crystallize from liquid Au/Ge droplets, whereas Ni-seeded Ge nanowire growth occurs at temperatures well below the Ni/Ge eutectic and nanowires evolve from a solid nickel germanide phase. A crystalline Ni_3Ge seed at the end of a Ge nanowire is shown in the TEM image in Figure 3c. It is noteworthy that the Ni_3Ge alloy has a relatively small lattice mismatch of less than 10% with Ge. One other difference between the two metals is that Au appears to catalyze DPG decomposition,[53] whereas there is no evidence that Ni does. MPS addition to the Ni-seeded nanowire reactions is needed to speed DPG decomposition enough to evolve high quality nanowires. The addition of MPS does not affect the Ni/Ge phase behavior—and nanowire growth still occurs from solid-phase seeds—but DPG decomposition becomes sufficiently fast in the presence of MPS to lead to nanowires with few crystal defects.

With sufficient reactant decomposition rates, one apparent advantage of solid-phase seeding compared to liquid-phase seeding appears to be less agglomeration of seed particles, as first reported by Tuan, et al.[43] The Ni-seeded nanowires (with MPS added) had a very narrow diameter distribution, much narrower than the nanowires produced with Au seeds. The average diameter of the Au-seeded Ge nanowires made in the presence of MPS was 40 nm. Thombare et al.[46] have also observed similar diameter-dependent differences in Ge nanowire growth from Ni seeds.

CONCLUSIONS

Ge nanowire synthesis using Ni nanocrystals as seeds can be carried out in supercritical toluene using DPG as a reactant. However, unlike Au, Ni seeds are rather poor catalysts for Ge nanowire growth—*unless* an additive is present to speed DPG decomposition. DPG decomposes by phenyl redistribution to germane and higher order phenylgermanes such as triphenylgermane and tetraphenylgermane. Ge incorporates into the nanowires by decomposition of germane, while TPG and QPG are unreactive. MPS was found to significantly enhance DPG decomposition and greatly improve Ge nanowire growth by withdrawing phenyl groups from DPG and serving as a phenyl sink to push the reaction product to germane. This enables the production of a high yield of straight nanowires with narrow diameters and narrow diameter distributions using Ni seeds.

This study highlights the essential role of reactant decomposition kinetics and control for making high quality nanowires. The seed metal and its interaction with the

dx.doi.org/10.1021/cm401047w | *Chem. Mater.* 2013, 25, 2172−2177

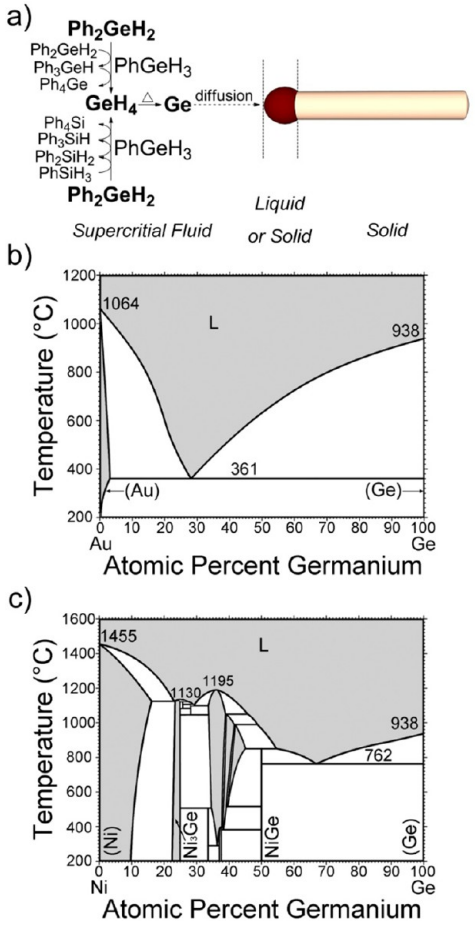

Figure 5. (a) DPG decomposition pathway with and without MPS. Ge nanowires form by SFLS or SFSS growth depending on whether the seed particles become liquid or remain solid. (b) Au–Ge[41] and (c) Ni–Ge[68] phase diagrams.

semiconductor are obviously influential, but the rate at which the semiconductor is fed to the seed particle is also extremely important.

■ ASSOCIATED CONTENT

Ⓢ Supporting Information

Experimental Details for Au and Ni nanocrystal synthesis, TEM images of Au and Ni nanocrystal seeds, SEM images of Ni-seeded nanowires synthesized at lower temperature, EDS compositional analysis. This material is available free of charge via the Internet at http://pubs.acs.org.

■ AUTHOR INFORMATION

Corresponding Author

*Phone: +1-512-471-5633. Fax: +1-512-471-7060. E-mail: korgel@che.utexas.edu.

Notes

The authors declare no competing financial interest.

■ ACKNOWLEDGMENTS

We acknowledge financial support from the Robert A. Welch Foundation (F-1494) and the Air Force Research Laboratory (FA-8650-07-2-5061). We also thank Vince Holmberg for helpful discussions and Karin Keller and Ian Riddington for assistance with GC-MS measurements.

■ REFERENCES

(1) Korgel, B. A. *AIChE J.* **2009**, *55*, 842–848.
(2) Trentler, T. J.; Hickman, K. M.; Goel, S. C.; Viano, A. M.; Gibbons, P. C.; Buhro, W. E. *Science* **1995**, *270*, 1791.
(3) Wang, F. D.; Dong, A. G.; Sun, J. W.; Tang, R.; Yu, H.; Buhro, W. E. *Inorg. Chem.* **2006**, *45*, 7511.
(4) Kuno, M. *Phys. Chem. Chem. Phys.* **2008**, *10*, 620–639.
(5) Holmes, J. D.; Johnston, K. P.; Doty, R. C.; Korgel, B. A. *Science* **2000**, *287*, 1471.
(6) Hanrath, T.; Korgel, B. A. *Adv. Mater.* **2003**, *15*, 437.
(7) Heitsch, A. T.; Fanfair, D. D.; Tuan, H. Y.; Korgel, B. A. *J. Am. Chem. Soc.* **2008**, *130*, 5436–5437.
(8) Tuan, H. Y.; Korgel, B. A. *Chem. Mater.* **2008**, *20*, 1239–1241.
(9) Hanrath, T.; Korgel, B. A. *J. Am. Chem. Soc.* **2002**, *124*, 1424–1429.
(10) Lu, X. M.; Fanfair, D. D.; Johnston, K. P.; Korgel, B. A. *J. Am. Chem. Soc.* **2005**, *127*, 15718–15719.
(11) Davidson, F. M., III; Schricker, A. D.; Wiacek, R. J.; Korgel, B. A. *Adv. Mater.* **2004**, *16*, 646–649.
(12) Davidson, F. M., III; Wiacek, R.; Korgel, B. A. *Chem. Mater.* **2005**, *17*, 230–233.
(13) Yu, H.; Buhro, W. E. *Adv. Mater.* **2003**, *15*, 416–419.
(14) Yu, H.; Li, J.; Loomis, R. A.; Wang, L.-W.; Buhro, W. E. *Nat. Mater.* **2003**, *2*, 517–520.
(15) Sun, J.; Buhro, W. E. *Angew. Chem.* **2008**, *120*, 3259–3262.
(16) Yu, H.; Li, J.; Loomis, R. A.; Gibbons, P. C.; Wang, L.; Buhro, W. E. *J. Am. Chem. Soc.* **2003**, *125*, 16168–16169.
(17) Grebinski, J. W.; Hull, K. L.; Zhang, J.; Kosel, T. H.; Kuno, M. *Chem. Mater.* **2004**, *16*, 5260–5272.
(18) Kuno, M.; Ahmad, O.; Protasenko, V.; Bacinello, D.; Kosel, T. H. *Chem. Mater.* **2006**, *18*, 5722–5732.
(19) Fanfair, D. D.; Korgel, B. A. *Chem. Mater.* **2007**, *19*, 4943–4948.
(20) Fanfair, D. D.; Korgel, B. A. *Chem. Mater.* **2008**, *8*, 3246–3252.
(21) Dong, A.; Wang, F.; Daulton, T. L.; Buhro, W. E. *Nano Lett.* **2007**, *7*, 1308–1313.
(22) Ouyang, L.; Maher, K. N.; Yu, C. L.; McCarty, J.; Park, H. *J. Am. Chem. Soc.* **2007**, *129*, 133–138.
(23) Wooten, A. J.; Werder, D. J.; Williams, D. J.; Casson, J. L.; Hollingsworth, J. A. *J. Am. Chem. Soc.* **2009**, *131*, 16177–16188.
(24) Steinhagen, C.; Akhavan, V. A.; Goodfellow, B. W.; Panthani, M. G.; Harris, J. T.; Holmberg, V. C.; Korgel, B. A. *ACS Appl. Mater. Interfaces* **2011**, *3*, 1781–1785.
(25) Wagner, R. S.; Ellis, W. C. *Appl. Phys. Lett.* **1964**, *4*, 89–90.
(26) Hu, J. T.; Odom, T. W.; Lieber, C. M. *Acc. Chem. Res.* **1999**, *32*, 435.
(27) Wang, D. W.; Dai, H. J. *Angew. Chem., Int. Ed.* **2002**, *114*, 4977–4980.
(28) Wu, Y. Y.; Yang, P. D. *J. Am. Chem. Soc.* **2001**, *123*, 3165–3166.
(29) Tutuc, E.; Appenzeller, J.; Reuter, M. C.; Guha, S. *Nano Lett.* **2006**, *6*, 2070–2074.
(30) Lensch-Falk, J. L.; Hemesath, E. R.; Perea, D. E.; Lauhon, L. J. *J. Mater. Chem.* **2009**, *19*, 849–857.
(31) Greytak, A. B.; Lauhon, L. J.; Gudiksen, M. S.; Lieber, C. M. *Appl. Phys. Lett.* **2004**, *84*, 4176–4178.
(32) Holmberg, V. C.; Panthani, M. G.; Korgel, B. A. *Science* **2009**, *326*, 405–407.
(33) Smith, D. A.; Holmberg, V. C.; Korgel, B. A. *ACS Nano* **2010**, *4*, 2356.
(34) Holmberg, V. C.; Rasch, M. R.; Korgel, B. A. *Langmuir* **2010**, *26*, 14241–14246.
(35) Holmberg, V. C.; Bogart, T. D.; Chockla, A. M.; Hessel, C. M.; Korgel, B. A. *J. Phys. Chem. C* **2012**, *116*, 22486–22491.
(36) Ngo, L. T.; Almécija, D.; Sader, J. E.; Daly, B.; Petkov, N.; Holmes, J. D.; Erts, D.; Boland, J. J. *Nano Lett.* **2006**, *6*, 2964–2968.
(37) Dayeh, S. A.; Picreaux, S. T. *Nano Lett.* **2010**, *10*, 4032–4039.
(38) Gamalski, A. D.; Tersoff, J.; Sharma, R.; Ducati, C.; Hofmann, S. *Nano Lett.* **2010**, *10*, 2972–2976.
(39) Wang, D.; Tu, R.; Zhang, L.; Dai, H. *Angew. Chem. Int. Ed.* **2005**, *44*, 2925–2929.

(40) Yang, H.-J.; Tuan, H.-Y. *J. Mater. Chem.* **2012**, *22*, 2215−2225.
(41) Okamoto, H.; Massalski, T. B. *Au-Ge (Gold-Germanium), Binary Alloy Phase Diagrams II Ed.* **1990**, *1*, 373−375.
(42) Dunlap, W. C. *Phys. Rev.* **1953**, *91*, 1282.
(43) Tuan, H.-Y.; Lee, D. C.; Hanrath, T.; Korgel, B. A. *Chem. Mater.* **2005**, *17*, 5705−5711.
(44) Tuan, H. Y.; Lee, D. C.; Korgel, B. A. *Angew. Chem., Int. Ed.* **2006**, *45*, 5184.
(45) Barth, S.; Kolesnik, M. M.; Dongegan, K.; Krstic, V.; Holmes, J. D. *Chem. Mater.* **2011**, *23*, 3335.
(46) Thombare, S. V.; Marshall, A. F.; McIntyre, P. C. *Appl. Phys. Lett.* **2012**, *112*, 054325.
(47) Chueh, Y.-L.; Fan, Z.; Takei, K.; Ko, H.; Kapadia, R.; Rathore, A. A.; Miller, N.; Yu, K.; Wu, M.; Haller, E. E.; Javey, A. *Nano Lett.* **2010**, *10*, 520−523.
(48) Geaney, H.; Dickinson, C.; Barrett, C. A.; Ryan, K. M. *Chem. Mater.* **2011**, *23*, 4838−4843.
(49) Kang, K.; Gu, G. H.; Kim, D. A.; Park, C. G.; Jo, M.-H. *Chem. Mater.* **2008**, *20*, 6577−6579.
(50) Kang, K.; Kim, D. A.; Lee, H.-S.; Kim, C.-J.; Yang, J.-E.; Jo, M.-H. *Adv. Mater.* **2008**, *20*, 4684−4690.
(51) Biswas, S.; Singha, A.; Morris, M. A.; Holmes, J. D. *Nano Lett.* **2012**, *12*, 5654−5663.
(52) Dřínek, V.; Fajgar, R.; Klementova, M.; Subrt, J. *J. Electrochem. Soc.* **2010**, *157*, K218−K222.
(53) Chockla, A. M.; Korgel, B. A. *J. Mater. Chem.* **2009**, *19*, 996−1001.
(54) Lee, D. C.; Hanrath, T.; Korgel, B. A. *Angew. Chem., Int. Ed.* **2005**, *44*, 3573.
(55) Yuan, F.-W.; Tuan, H.-Y. *Cryst. Growth Des.* **2010**, *10*, 4741−4745.
(56) Yang, H.-J.; Yuan, F.-W.; Tuan, H.-Y. *Chem. Commun.* **2010**, *46*, 6105−6107.
(57) Geaney, H.; Mullane, E.; Ramasse, Q. M.; Ryan, K. M. *Nano Lett.* **2013**, *13*, 1675−1680.
(58) Mullane, E.; Kennedy, T.; Geaney, H.; Dickinson, C.; Ryan, K. M. *Chem. Mater.* **2013**, DOI: 10.1021/cm400367v.
(59) Coleman, N. R. B.; O'Sullivan, N.; Ryan, K. M.; Crowley, T. A.; Morris, M. A.; Spalding, T. R.; Steytler, D. C.; Holmes, J. D. *J. Am. Chem. Soc.* **2001**, *123*, 7010−7016.
(60) Brust, M.; Walker, M.; Bethell, D.; Schiffrin, D. J.; Whyman, R. *Chem. Commun.* **1994**, 801.
(61) Park, J.; Kang, E.; Son, S. U.; Park, H. M.; Lee, M. K.; Kim, J.; Kim, K. W.; Noh, H. J.; Park, J. H.; Bae, C. J.; Park, J. G.; Hyeon, T. *Adv. Mater.* **2005**, *17*, 429.
(62) Holmberg, V. C.; Korgel, B. A. *Chem. Mater.* **2010**, *22*, 3698.
(63) Hanrath, T.; Korgel, B. A. *J. Am. Chem. Soc.* **2004**, *126*, 15466.
(64) Hanrath, T.; Korgel, B. A. *Small* **2005**, *1*, 717−721.
(65) Chockla, A. M.; Harris, J. T.; Korgel, B. A. *Chem. Mater.* **2011**, *23*, 1964.
(66) Werner, D. *The Biology of Diatoms*; University of California Press: Berkeley and Los Angeles, 1977; Chapter 4.
(67) MPS and MPG are not observed in the spectra because the retention time of MPS or MPG is very close to toluene (∼3 s). Data are collected only after 5 s.
(68) Nash, A.; Nash, P. *Ge−Ni (Germanium-Nickel), Binary Alloy Phase Diagrams II Ed.* **1990**, *2*, 1974−1976.